Presented at the 5th Conference on Mathematics and Computers in Sport, G. Cohen, Editor, University of Technology, Sydney, New South Wales, Australia, 14-16 June 2000.

SIMULATION OF FRISBEE FLIGHT

M. Hubbard and S. A. Hummel *
Department of Mechanical and Aeronautical Engineering
University of California, Davis
CA 95616 USA

Abstract

Flight equations of motion of the Frisbee are presented. Few reports of aerodynamic force and moment coefficients are available in the literature. Aerodynamic coefficients are estimated using parameter identification by matching predicted and experimental trajectories of markers on the disc. RMS errors as small as 1.4 mm are achieved between predicted and measured marker positions in flights of about 2 m. Longer flights are calculated but performance is very sensitive to the aerodynamic coefficients.

1 Introduction

The Frisbee was invented in 1948. Since then it has enjoyed remarkable popularity. Today it is used by millions as a recreational toy and by thousands in the sport of Ultimate Frisbee. Despite its popularity there is relatively little scientific and technical information in the literature documenting the dynamics and aerodynamics of the implement. The book by Johnson [6] is a practitioners' handbook which includes information on the history of the Frisbee, Frisbee games and throwing techniques. Two brief, somewhat anecdotal, descriptions of the flight dynamics and aerodynamics for the informed layman have been provided by Bloomfield [2] and Schuurmans [12].

A study of a self suspended Frisbee-like flare was conducted by Stilley [14]. This work included spinning and non-spinning wind tunnel tests, computer simulations of flight, and experimental flight tests of three disc configurations. A main conclusion was that the effect of spin on the aerodynamic forces is small. Stilley hypothesized, but did not measure, a "Magnus rolling moment", induced by the interaction of spin and velocity. Stability criteria were presented involving relations between the stability derivatives. Mitchell [9] measured the lift and drag forces on three different Frisbees over a range of speeds and angles of attack. He confirmed the observation of Stilley [14] that spin affects lift and drag only little, but did not measure pitching moment.

Recently Potts and Crowther [11] studied the aerodynamics more completely. They accurately measured lift and drag forces and pitching and rolling moment as a function of Reynolds number and spin parameter, the ratio of speed at the edge of the disc due to spin to the speed of the center. They corroborated the results of Stilley and Carstens [15] at zero spin. Slight differences in lift force and pitching moment were attributed to the different cross sectional shapes and thickness ratios of the Frisbees tested from those of Stilley and Carstens. Potts and Crowther found little effect of Reynolds number on lift and drag except at high angles of attack ($\alpha \geq 20$ deg). Although they detected virtually no effect of spin parameter on lift and drag, non-zero rolling moments and small but distinct effects of spin parameter on pitching and rolling moments were observed.

In related work, Soong [13] analyzed the dynamics of the discus throw, those shape differs from that of the Frisbee mainly in that it has a plane as well as an axis of symmetry. Soong did not include any rolling

* This paper was partially researched and prepared while participating in an Ultimate Frisbee tournament in Hawaii. The author is grateful for the hospitality shown by all

aerodynamic moments and showed that the main effect of pitching moment is to cause a precession of the spin in roll, thus decreasing lift later in the flight.

Frohlich [4] also investigated the flight dynamics of the discus. With computer simulations that relied on discus lift and drag coefficients determined experimentally by Ganslen [5] and others, he showed that the discus can be thrown farther against the wind than with it. Although this paper included a complete discussion of the effects of aerodynamic moments on the subsequent flight, the analysis remains somewhat hypothetical because of the absence of any experimental data on pitching and rolling aerodynamic moments. Frohlich also noted the remarkable similarity between the discus and the Frisbee.

The present paper presents a three-dimensional mathematical model of Frisbee flight including the translational and rotational dynamics of the disc driven by the aerodynamic forces and moments caused by the motion. The aerodynamic coefficients used in the model are estimated using experimental flight data. These are also compared to values of similar coefficients from the literature.

2 Flight dynamics

The Frisbee is assumed to be an axially symmetric rigid body with mass m and axial and diametral mass moments of inertia I_a and I_d, respectively. Several reference frames are used in the development of the equations. The Frisbee centre of mass (cm) is assumed to be located at coordinates xyz in an inertial reference frame N with the xy plane horizontal and the direction of the x axis chosen (arbitrarily) so that the initial (or release) velocity vector $\boldsymbol{v}$ of the centre of mass lies near the xz plane.

A body-fixed reference frame C (see Fig. 1) has its origin at the mass center and its $\boldsymbol{c_1c_2}$ plane parallel to the plane of the disc. The general orientation of the Frisbee (and of the C frame) in the N frame is achieved through three successive Euler angle rotations (a 123 Euler angle set). As shown in Fig. 1, first the N frame is rotated about its $\boldsymbol{n_1}$ axis through angle ϕ to reach the intermediate A frame. Next the A frame is rotated about the $\boldsymbol{a_2}$ axis through angle θ to reach a second intermediate frame B. Finally the B frame is rotated about its $\boldsymbol{b}_3$ axis through angle γ to reach the body-fixed C frame. In the derivation of the equations of motion below we often express vectors in the B frame. The three Euler angles ϕ, θ and γ determine the general orientation of the disc. Only ϕ and θ are involved in the transformation matrix T relating the N and frames,

$$T = \begin{bmatrix} \cos\theta & 0 & \sin\theta \\ \sin\theta\sin\phi & \cos\phi & -\cos\theta\sin\phi \\ -\sin\theta\cos\phi & \sin\phi & \cos\theta\cos\phi \end{bmatrix}$$

The angular velocity of the disc relative to the inertial N frame is given by

$$\boldsymbol{\omega} = \phi' \cos\theta\, \mathbf{b}_1 + \theta'\, \mathbf{b}_2 + (\phi' \sin\theta + \gamma')\, \mathbf{b}_3.$$

In the general flight configuration, the velocity of the center of mass is written as

$$\boldsymbol{v} = u\mathbf{b}_1 + v\mathbf{b}_2 + w\mathbf{b}_3$$

consistent with the typical procedure followed in analyses of flight vehicles (Etkin and Reid [3]).

The equations of motion, the details of which are summarized in the Appendix, are a Newton-Euler description of the motion of a rigid body. These are expressed in the B frame since, because of symmetry, B is (as well as C) a set of principal axes of inertia for the disc. The equations in vector form are given by

$$\mathbf{F} = m\,(d\boldsymbol{v}/dt + \boldsymbol{\omega}_\mathbf{b} * \boldsymbol{v})$$

$$\mathbf{M} = \mathrm{I}d\boldsymbol{\omega}/dt + \boldsymbol{\omega}_\mathbf{b} * \mathrm{I}\boldsymbol{\omega}$$

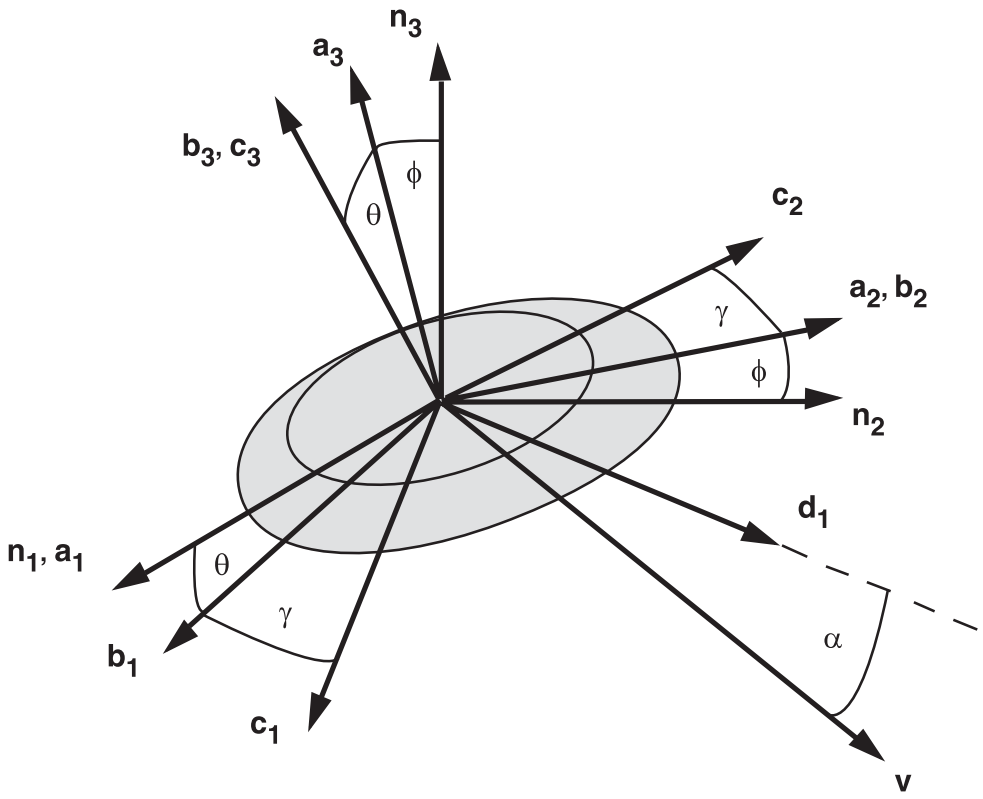

Figure 1: A Frisbee body-fixed reference frame is attained with a 123 Euler angle set of rotations.

where **F** and **M** are the aerodynamic and gravitational forces and moments applied to the disc, respectively, $\boldsymbol{\omega}_\mathbf{b}$ is the angular velocity of the B frame relative to N, and I is the moment of inertia matrix

$$I = \begin{bmatrix} I_d & 0 & 0 \\ 0 & I_d & 0 \\ 0 & 0 & I_a \end{bmatrix}$$

3 Aerodynamic forces and moments

3.1 Forces

The natural directions for decomposition of the aerodynamic forces are determined by the velocity (see Fig. 2). Let the unit vector along the projection of $\boldsymbol{v}$ on the $\boldsymbol{b_1 b_2}$ disc plane be denoted by $\boldsymbol{d_1}$. Assuming $\boldsymbol{d_3}$ (= $\boldsymbol{b_3}$) is perpendicular to the plane of the disc, we let $\boldsymbol{d_2} = \boldsymbol{d_3} \times \boldsymbol{d_1}$. The angle of attack α is defined as the angle between $\boldsymbol{v}$ and $\boldsymbol{d_1}$. We assume that the two components of the aerodynamic force along and perpendicular to $\boldsymbol{v}$ in the $\boldsymbol{d_1 d_3}$ plane (called the lift L and drag D, respectively) are each functions of lift and drag coefficients in the standard way:

$$L = C_l A \rho v^2 / 2, \qquad D = C_d A \rho v^2 / 2,$$

where here v denotes the magnitude of v (not to be confused with the $\boldsymbol{b_2}$ component of $\boldsymbol{v}$ in Eq. 2), ρ is the air density, and A is the projected or planform area of the disc. The lift and drag coefficients C_l and C_d are further assumed (for small angles of attack) to be given by the expressions

$$C_l = C_{l\mathrm{o}} + C_{l\alpha}\,\alpha, \qquad C_d = C_{d\mathrm{o}} + C_{d\alpha}\,\alpha^2.$$

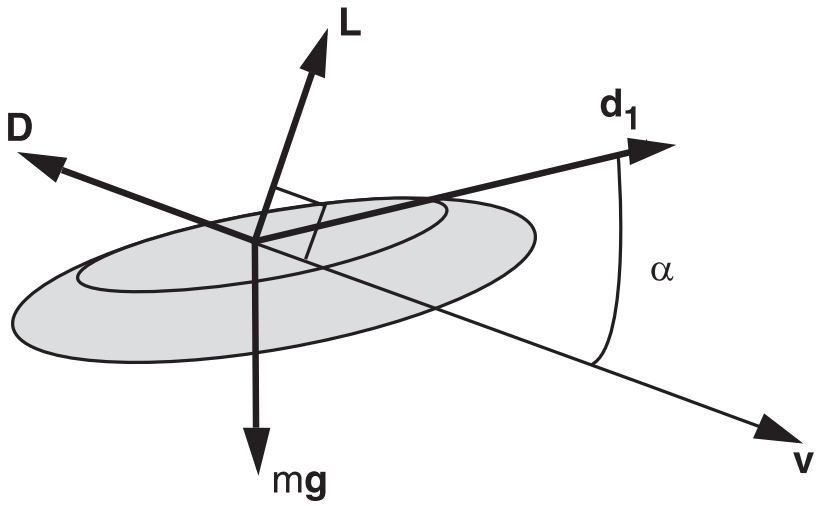

Figure 2: Drag and lift forces act along and perpendicular to the velocity vector $\boldsymbol{v}$ and are functions of α, the angle between $\boldsymbol{v}$ and $\boldsymbol{d_1}$ in the disc plane.

The forms of the relations for L and D above are consistent with the general findings of several researchers that spin does not affect L and D to first order (McShane, et al. [8], Stilley [14], Mitchell [9]). Note that the lift is linear in α while drag dependence is quadratic. Although this form is exact for a symmetric airfoil, the formulation of Potts and Crowther [11] is probably more accurate in that it predicts the minimum drag to occur at the zero-lift angle of attack, which they measure to be about -4 deg.

It is important to remember that the four coefficients above are chosen (in contrast to using measured forces) for purposes of simplicity and efficiency. This description provides a more practical version of the dependence of the forces on angle of attack, at some cost in accuracy.

Were the lateral projected area of the Frisbee (in the $\boldsymbol{d_1 d_3}$ plane) larger compared to its planform area, it would be important to include a third $\boldsymbol{d_2}$ component of the aerodynamic force. For example, in the flight of spherical balls (Alaways and Hubbard [1]) the Robins-Magnus lift force produced by the circulation due to spin about the $\boldsymbol{d_3}$ axis is important, but this force is neglected here. Thus the four constant coefficients C_{lo}, $C_{l\alpha}$, C_{do}, $C_{d\alpha}$ are assumed here to be a simplified but complete parametric description of the force-producing capability of the disc. Decomposing the lift and drag into the D frame gives an expression for the aerodynamic force

$$\mathbf{F} = L \sin\alpha - D \cos\alpha)\, \boldsymbol{d_1} + L \cos\alpha + D \sin\alpha)\, \boldsymbol{d_3}.$$

3.2 Moments

The net aerodynamic force acts at the centre of pressure (cp) which, in general, does not coincide with the centre of mass. Thus it also exerts a moment about the cm. One of the components is a pitching moment about the $\boldsymbol{d_2}$ axis of the form

$$M_2 = Ad\rho v^2 \, (C_{M\,\alpha}\,\alpha \;+\; C_{M\,\alpha'}\,\alpha' \,) / 2$$

where the angular stiffness and damping coefficients $C_{M\,\alpha}$ and $C_{M\,\alpha'}$, respectively, are constants and $\boldsymbol{d}$ is the diameter of the disc.

For an axisymmetric non-spinning disc, the cp would lie in the $\boldsymbol{d_1 d_3}$ plane. However, the nonzero spin causes the position of the cp to have a small $\boldsymbol{d_2}$ component as well. The coefficient $C_{R\,\gamma'}$ models this effect (called the "rolling Magnus moment" by Stilley, [14]) and assumes that a part of the $\boldsymbol{d_1}$ component of the moment is proportional to the spin γ'. A physical explanation of this coefficient is the small effect the spin has on the rotation of the mean flow separation line away from the $\boldsymbol{d_2}$ direction. Its magnitude is typically very small. Potts and Crowther [11] have shown that this coefficient is significantly different from zero only at

small angles of attack $\alpha \leq 10$ deg. The previously introduced damping coefficient $C_{M\,\alpha'}$ also relates the $\boldsymbol{d_1}$ component of disc angular velocity to the other part of the moment in the $\boldsymbol{d_1}$ direction yielding

$$M_1 = Ad\rho v^2 \left(C_{R\gamma'}\,\gamma' + C_{M\alpha'}\,\boldsymbol{\omega}\cdot\boldsymbol{d_1}/2\right).$$

Finally there is a spin-deceleration torque which acts along the $\boldsymbol{d_3}$ axis. This torque differs fundamentally from the $C_{M\alpha'}$ term in M_2, for example, in that it is due to viscous shear stresses in the fluid rather than from a displacement of the cp from the cm. It is assumed to be proportional to the $\boldsymbol{d_3}$ component of the disc angular velocity $\phi' \sin\theta + \gamma'$ through the spin-down coefficient $C_{N\,r}$

$$M_3 = C_{N\,r}\left(\phi' \sin\theta + \gamma'\right).$$

Justification for a functional dependence of $C_{N\,r}$ on α can be found in Stilley [14] (and Nielsen and Synge [10]), which is here neglected. Combining the three components of the aerodynamic moments above yields

$$\boldsymbol{M} = M_1\boldsymbol{d_1} + M_2\boldsymbol{d_2} + M_3\boldsymbol{d_3}.$$

In summary, the aerodynamic forces and moments are parameterized by the eight coefficients shown in the heading of Table 1.

3.3 Evaluation of coefficients

The experimental evidence in the literature for the values of these aerodynamic force and moment coefficients is scanty and incomplete. Stilley [14] contains wind tunnel results for lift, drag and pitching moment as a function of angle of attack for a single Frisbee. Mitchell [9] measured lift and drag coefficients in the range of angles of attack $-20 \leq \alpha \leq 20$ deg for three different frisbees in a wind tunnel over the range of speeds $2.7 \leq v \leq 28.2$ m/sec. Mitchell also found that spin did not affect the lift and drag forces substantially, but he did not measure pitching moment and thus provided no information regarding the moment coefficients $C_{M\,\alpha}$, $C_{M\,\alpha'}$, $C_{R\,\gamma'}$ and $C_{N\,r}$. The recent, more detailed work of Potts and Crowther [11] does give measurements of pitching and rolling moments. However, wind tunnel tests must be essentially quasi-static, and consequently no experimental evidence is available on the dependence of forces and moments on angular velocities.

In another approach, approximations of the aerodynamic coefficients may be obtained from flight data. Three small circular reflective markers were attached to the top of the Frisbee and their three dimensional inertial coordinates tracked during flights using high speed (120 Hz) video. Estimates of the aerodynamic coefficients, together with initial conditions for the short experimental flight, were determined iteratively by modifying the aerodynamic coefficients and initial conditions in a simulation to minimize the differences between predicted and measured marker positions. Coefficients for two flights are shown in Table 1.

Flight	C_{lo}	$C_{l\alpha}$	C_{do}	$C_{d\alpha}$	$C_{M\,\alpha}$	$C_{M\alpha'}$ sec	$C_{R\,\gamma'}$ sec	$C_{N\,r}$ N-m-sec
fssh3	-0.40	1.89	0.83	0.83	-0.16	0.029	0.012	0.000074
bffl8	1.17	0.28	5.07	0.077	0.22	0.025	-0.0030	-0.00000025

Table 1: Aerodynamic force and moment coefficients for two flights.

Figure 3 shows the projections in the horizontal *xy* plane of the predicted and measured marker trajectories for flight fssh3. The disc makes almost one complete revolution and the marker trajectories superimpose nearly harmonic motion in *x* and *y* on the mean motion of the cm. Figure 4 shows the residuals, the differences between the measured and predicted positions of the three markers, arrayed end-to-end. Even

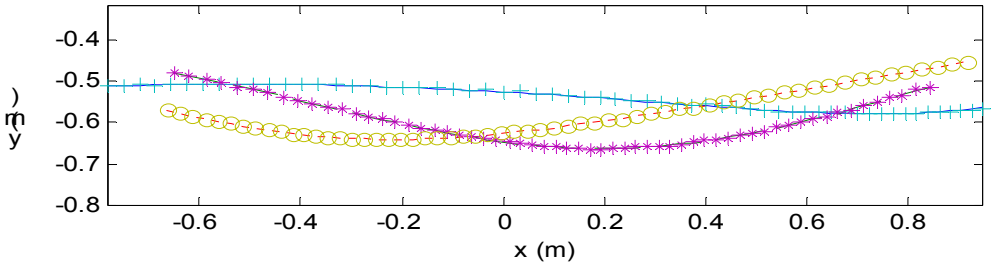

Figure 3: Predicted (lines) and measured (symbols) *x* and *y* positions for three markers in flight fssh3.

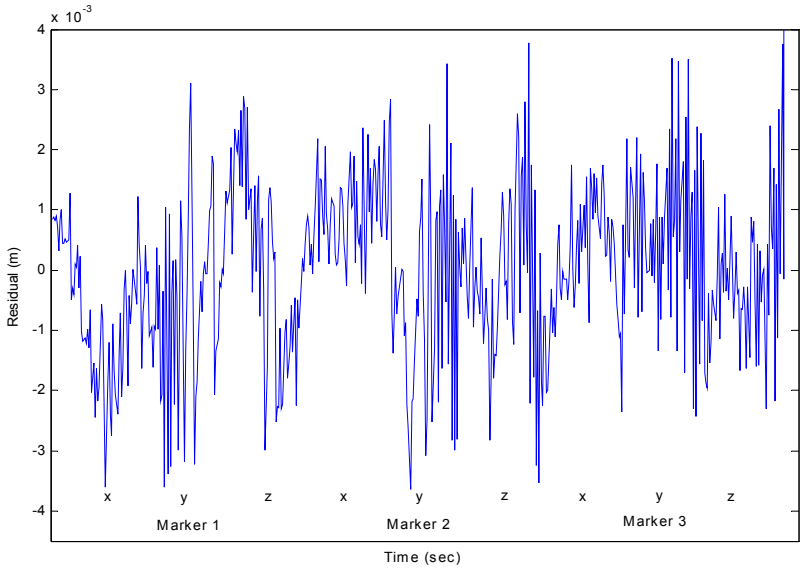

Figure 4: Prediction errors in x, y, and z for three markers in flight fssh3 have an rms of only 1.4 mm.

though the root mean squared (rms) error in the prediction is only 1.4 mm over the course of the 2 m long flight and the residuals are nearly white, there is some obvious correlation present indicating that a more completely descriptive model of the flight might be possible, including possibly a more accurate drag parameterization. The aerodynamic coefficients determined from the flight portrayed in Figs. 3 and 4 are shown in the first row of Table 1. Coefficients from a second flight are shown in the second row. There exist frisbees of many sizes and cross-sectional shapes, and certainly with correspondingly different aerodynamic coefficients, but a single Frisbee was used in all our flight experiments. Even though one would expect the coefficients from two flights of the same disc to be nearly equal, as seen in Table 1 this was not the case. It is curious that the more typical (in the sense discussed below) flight bffl8 yields unlikely and in some cases physically impossible coefficients, while the less typical flight fssh3 produces coefficients that are more similar to those found in the wind tunnel experiments discussed above.

This suggests a modified procedure for the identification of the aerodynamic coefficients in the future. Rather than identifying a different set of coefficients for each flight, a single set of coefficients may be determined which allow a best fit of the marker data from numerous flights, covering a wide range of initial conditions.

It is also worthwhile to note the sensitivity of the identified coefficients to noise in the experimentally measured marker positions. Small errors can require unrepresentative, or in some cases even physically

impossible, values of coefficients to yield dynamics which will fit the data. This has apparently happened in the second of the flights in Table 1, which yielded a negative, but still extremely small, value for $C_{N\,r}$ implying that the spin actually increased very slightly during the flight rather than decreasing. Similar unreasonable estimates of negative drag coefficients have occurred in cases involving errors in measured x position that required the velocity to increase in flight. Thus an essential requirement for this technique of coefficient identification is very accurate marker position data. In addition, flight times are required that are long enough to make the effects of the coefficients apparent through the dynamics.

Parameter	m	I_a	I_d	d	A	ρ	g
	Kg	Kg-m^2	Kg-m^2	m	m^2	Kg-m^3	m /sec^2
	0.175	0.00197	0.00138	0.269	0.057	1.23	9.7935

Table 2: Values of non-aerodynamic simulation parameters.

In the simulations of two flights presented below we assume the aerodynamic force and moment coefficients are those given in the two rows of Table 1. Table 2 contains the non-aerodynamic parameters for the test Frisbee which are also the parameters for the simulations discussed below. The mass, in particular, is relatively large compared to typical recreational discs, and is the official weight of discs used in Ultimate Frisbee competition.

Flight	x_0	y_0	z_0	u_0	v_0	w_0	ϕ_o	θ_o	γ_o	ϕ_o‘	θ_o‘	γ_o‘
	m	m	m	m /sec	m /sec	m /sec	rad	rad	rad	rad/sec	rad/sec	rad/sec
fssh3	-0.71	-0.52	1.13	3.03	-0.45	-2.25	-0.066	-0.34	3.01	-3.03	-0.76	-8.91
bffl8	-1.42	-0.40	0.81	8.40	-0.15	-1.23	-0.08	-0.25	4.40	-6.33	0.37	-37.1

Table 3: Initial conditions for two flights.

4 Simulation results

Shown in Fig. 5 are time histories of eleven of the twelve state variables ($x\ y\ z\ u\ v\ w\ \phi\ \theta\ \gamma\ \phi'\ \theta'\ \gamma'$) for an atypical right hand, backhand-thrown flight of about 0.5 sec. The initial conditions for this flight are shown in the first row of Table 3. This is a simulation of a flight which corresponds to that shown in Figs. 3 and 4. The disc was thrown rather slowly, with a velocity of 3.77 m/sec, and with a relatively small spin (8.91 rad/sec) and artificially large initial angle of attack. The disc was released 1.13 m from the ground and fell 1.04 m within 0.5 sec. The small dynamic pressure (of the order of 10 Pa) makes the aerodynamic forces relatively insignificant compared to the weight and results in a nearly parabolic fall. During the flight it traveled 1.62 m in the x direction, curving slightly right (in y) of the mean direction and then back again to the left. Because of the large initial angle of attack, the component of velocity perpendicular to the disc plane, w, is larger than the vertical component of velocity z'. The reader should recall that the velocities shown in part b) of Fig. 5 are components referred to the disc plane and are not the derivatives of x, y, and z in part a).

The disc was initially oriented with its far (away from the thrower) edge tilted downward, ϕ = - 0.065 rad, and the leading edge tilted upward, θ = - 0.34 rad. These angles changed significantly over the course of the flight. However, the angular velocity time histories, ϕ' and θ', indicated some signs of damping. Because the duration of the flight was so small compared to the characteristic time of spin decay (about 7 sec), the Frisbee lost only about 10 % of its initial spin rate of -8.91 rad/sec.

Shown in Fig. 6 are the same eleven state variables for a more typical flight than Fig. 5 (i.e. larger initial velocity and spin rate and smaller initial angle of attack). A simulation of 1.0 sec was created using the measured coefficients from flight bffl8 (see Table 2). The initial conditions for this flight are listed in Table 3. In this flight the dynamic pressure is more than four times that of the flight shown in Fig. 5. As a result the

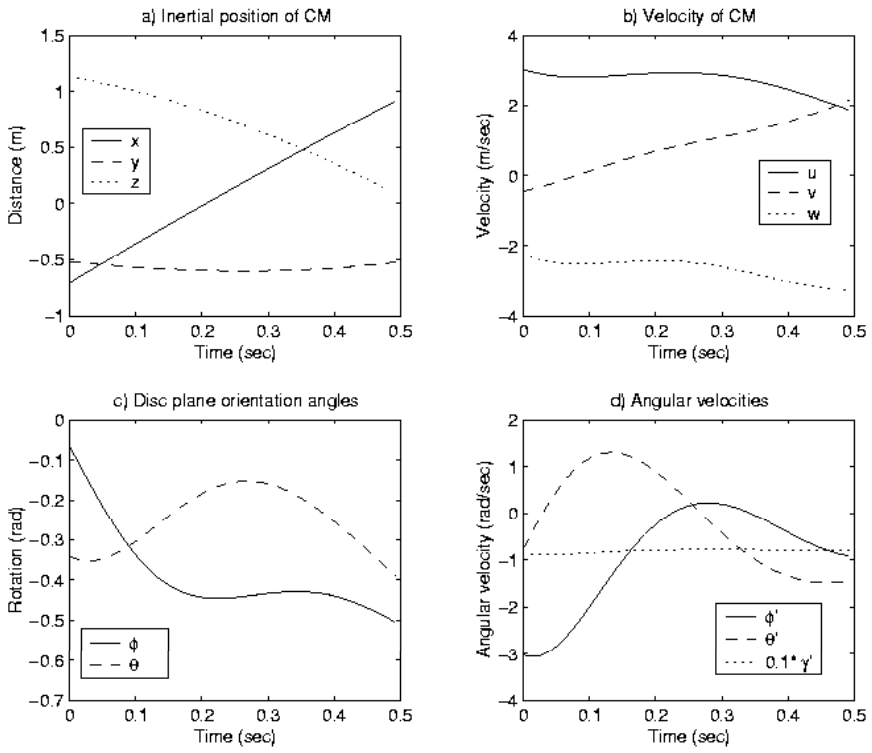

Figure 5: State variables versus time for flight fssh3 of Figs.3 and 4 and aerodynamic parameters from row 1 of Table1

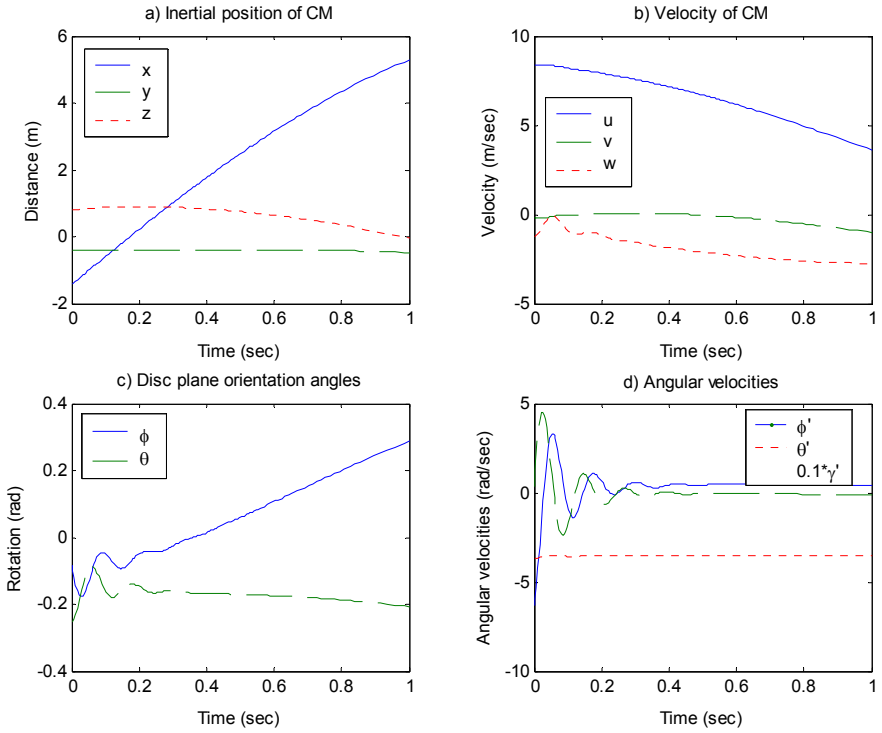

Figure 6: State variables versus time for extended flight bffl8.

characteristic times of response are correspondingly reduced and the mean aerodynamic force more nearly equals the weight. The inertial x coordinate increased roughly at the thrown speed of 8.48 m/sec and the Frisbee traveled 6.71 m. The inertial z coordinate increased initially but began to decrease after approximately 0.2 sec and underwent a net drop of 0.84 m. The y component of the disc mass center remained relatively constant. The disc was initially spinning at $\gamma' = -37.1$ rad/sec but this decreased to $\gamma' = -35.4$ rad/sec over the duration of the flight. Initially the far edge of the disc was tilted down, $\phi = -0.081$ rad, and the leading edge was tilted up at $\theta = -0.25$. For about the first 0.3 sec the angular velocities ϕ' and θ' underwent damped oscillations. Decreasing attitude oscillations such as these can frequently be observed with the naked eye. After the early oscillations subsided, ϕ then gradually increased through the flight to $\phi = 0.29$ rad. The leading edge continued to tilt up as θ decreased to -0.21 rad.

5 Conclusions

The equations of motion of Frisbee flight have been presented. Numerical solutions of these equations can provide quantitative flight information but are sensitive to the coefficients relating body orientation and translational and angular speeds to the aerodynamic forces and moments. Simulations of this type can provide a means for creating sets of initial conditions which produce flights with certain desirable characteristics. For example, in game situations one may use throws with sharp curvature in one direction or another since these may be advantageous from a tactical point of view. Alternatively a throw may be desired which hangs or flares over or near a given point on the field. Throws such as these may be investigated and ``designed" using the simulation techniques described herein.

Further work is needed in making the estimates of the aerodynamic coefficients from flight data more reliable and meaningful and perhaps in creating more complex parametric descriptions of the aerodynamics. This will require considerably longer experimental flights and more accurate kinematic data acquisition techniques. In addition, the use of data from a wide variety of flight conditions will make the identified coefficients more representative of the dynamic behavior of the Frisbee over a similarly broad flight regime.

References

[1] L. W. Alaways and M. Hubbard, "Experimental determination of baseball spin and lift", *J. Sports Sciences*, submitted.

[2] L. A. Bloomfield, "The flight of the Frisbee", *Sci. Am*., April (1999), 132.

[3] B. Etkin and L. D. Reid, *Dynamics of Flight: Stability and Control*, John Wiley & Sons (1996).

[4] C. Frohlich, "Aerodynamic effects on discus flight", *Am. J. of Phys*., **49** (1981), 1125-1132.

[5] R. V. Ganslen, "Aerodynamic and mechanical forces in discus flight" *Athletic J.* **44** (1964), 50.

[6] S. E. D. Johnson, *Frisbee: A Practitioner's Manual and Definitive Treatise*, Workman Publishing Company (1975).

[7] P. Katz, "The free flight of a rotating disc", *Israel J.Tech.*, **6** (1-2) (1968), 150-155.

[8] E. J. McShane, J. L. Kelly, and F. V. Reno, *Exterior Ballistics*, The University of Denver Press (1953).

[9] T. L. Mitchell, "The aerodynamic response of airborne discs", MS Thesis, University of Nevada, Las Vegas (1999).

[10] K. L. Nielsen and J. L. Synge, "On the motion of a spinning shell", *Q. Appl. Math*, **4** (1946), 201-226.

[11] J.R. Potts and W.J. Crowther, "The flow over a rotating disc-wing", RAeS Aerodynamics Research Conference Proceedings, London, U.K., April (2000).

[12] M. Schuurmans, "Flight of the Frisbee", *New Scientist*, July 28, **127** (1727) (1990), 37-40.

[13] T.-C. Soong, "The dynamics of discus throw", *J. appl. Mech*., **98** (1976), 531-536.

[14] G. D. Stilley, "Aerodynamic analysis of the self sustained flair", RDTR no. 199, Naval Ammunition Depot, Crane, Indiana (1972).

[15] G. D. Stilley and D. L. Carstens, "Adaptation of Frisbee flight principle to delivery of special ordnance", AIAA paper 72-982, (1972).

A Equations of motion

In the derivation of the equations of motion, the aerodynamic forces and moments originally expressed in frame D in Eqs. 5 and 6 are transformed to the B frame by multiplying by the transformation matrix T_2 relating B to D

$$\mathbf{F_b} = T_2\,\mathbf{F} \qquad \mathbf{M_b} = T_2\,\mathbf{M}$$

where

$$T_2 = \begin{bmatrix} \cos\beta & -\sin\beta & 0 \\ \sin\beta & \cos\beta & 0 \\ 0 & 0 & 1 \end{bmatrix}$$

and where β is the angle between the $\boldsymbol{b_1}$ and $\boldsymbol{d_1}$ axes

$$\beta = \arctan(v/u).$$

Then the differentiations in Eqs3 and 4 are carried out and the scalar components are solved for the accelerations yielding

$$u' = (F_{b1} - w\,\theta' + v\,\phi'\sin\theta)/m$$

$$v' = (F_{b2} + w\,\phi'\cos\theta - u\,\phi'\sin\theta)/m$$

$$w' = (F_{b3} + u\,\theta' - v\,\phi'\cos\theta)/m$$

$$\phi'' = (M_{b1} + 2\,I_d\,u\,\phi'\theta'\sin\theta - I_a\,\theta'\,\phi'\sin\theta + \gamma')\cos\theta)/I_d\cos\theta$$

$$\theta'' = (M_{b2} - I_d\,\phi'^2\cos\theta\sin\theta + I_a\,\phi'\cos\theta\,\phi'\sin\theta + \gamma')\,)/I_d$$

$$\gamma'' = (M_{b3} - I_a(\phi''\sin\theta + \phi'\,\theta'\cos\theta\cos\theta)/I_a$$

Finally, the velocity vector $\boldsymbol{v}$ with components u, v and w in the B frame is transformed into the N frame by multiplying by the transformation matrix T from Eq. 1 to give the rates of change of the inertial coordinates.

$$x = u\cos\theta + w\sin\theta$$

$$y = u\sin\theta\sin\phi + v\cos\phi - w\cos\theta\sin\phi$$

$$z = -u\sin\theta\cos\phi + v\sin\phi + w\cos\theta\cos\phi$$